Supplemental Information for

High-affinity metal binding by the *Escherichia coli* [NiFe]-hydrogenase accessory protein HypB is selectively modulated by SlyD

Mozhgan Khorasani-Motlagh[1], Michael J. Lacasse[1], Deborah B. Zamble[1,2*]

Supplemental Methods

Chemical cross-linking

Zn(II)-HypB or Ni(II)-E9A-HypB (20 μM) and SlyD or SlyD146 (80 μM) were incubated together for 3 h at 4°C in an anaerobic glovebox (95% N_2, 5% H_2) in protein buffer (25 mM HEPES, pH 7.5, 200 mM NaCl). EDC (1-Ethyl-3-[3-dimethylaminopropyl]carbodiimide hydrochloride, 5 mM) was added to Zn(II)-HypB, Ni(II)-E9A, SlyD, SlyD146 and allowed to react at room temperature for 1 h. Samples were then subjected to SDS-PAGE on 12.5% polyacrylamide gels and stained with Coomassie Blue.

Circular dichroism (CD) spectroscopy

WT-HypB and E9A-HypB were prepared for CD spectroscopy by diluting the protein in MilliQ water to a final concentration of approximately 10 μM in an anaerobic glovebox. The CD spectra were collected on a Jasco J-710 spectropolarimeter by scanning in the wavelength range of 190−260 nm at room temperature. Spectra were collected at 1 nm intervals with a scan speed of 20 nm/min. The final spectra obtained are averages of three scans and corrected by subtracting the background buffer signal. The observed ellipticity was converted into mean residue ellipticity ($[\theta]_{mre}$; deg cm^2dmol^{-1}).[1]

Supplemental Results

SlyD or SlyD146 and Zn(II)-HypB interact.

To check for complex formation between Zn(II)-HypB and SlyD a chemical cross-linking assay was used. Zn(II)-HypB (20 μM) and SlyD (80 μM) were incubated together with EDC, a water soluble carbodiimide zero-length cross-linker. Samples were monitored by SDS-PAGE gels and a cross–linked dimer was observed between Zn(II)-HypB and SlyD, indicating the protein–protein interaction (Fig. S4). To examine the role of the C-terminal tail of SlyD, the assay was repeated with SlyD146 and the result shows that removal the C-terminal tail of SlyD did not prevent the interaction with Zn(II)-HypB (Fig. S4). This result is consistent with complex formation observed with Ni(II)-HypB.[2]

Molecular modeling of E9A

An *in silico* mutagenesis of Glu9 to Ala was performed to probe changes in the optimized geometry. Since the E9A mutation did not change the coordination of nickel, molecular modeling was applied to predict the Zn(II)-E9A-HypB site. A variety of conditions were used, including protonation of the terminal amine and the presence of one, two, or three water molecules to fill empty coordination sites. If the terminal amine was protonated, Zn(II)-E9A-B9 tended to adopt a tetrahedral geometry with one site occupied with water. This result was not consistent with the XAS analysis that suggested a 5-coordinate S_3/O_2 geometry. However, with a neutral terminal amine available for coordination (neutral), zinc adopted a 5-coordinate square pyramidal geometry with water in the axial position, suggesting that Zn(II)-E9A-HypB terminal amine might be involved in zinc coordination. It is also possible that in the context of the full-length protein Zn(II)-E9A-HypB recruits other residues that are not included in the peptide maquette used for computation.

Supplemental Figures

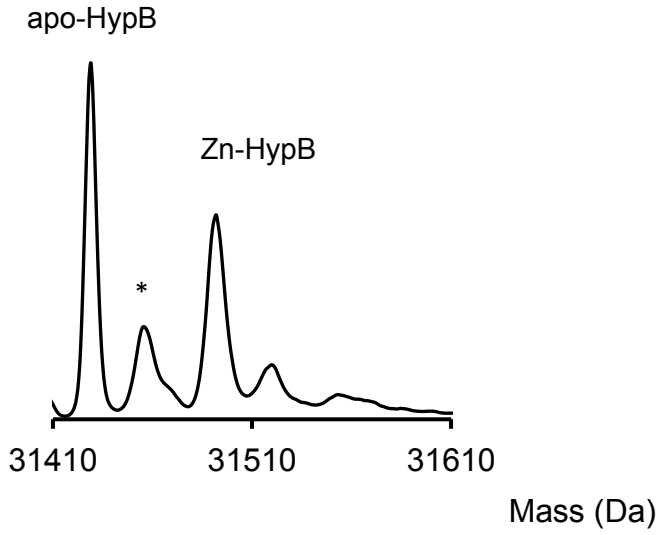

Supplemental Figure 1. Reconstructed mass spectrum of apo-HypB incubated with one equivalent of Zn(II). The relative peak intensity of Zn(II)-HypB to apo-HypB is ~ 0.8. The asterisk indicates apo-HypB with a previously-observed +28 Da modification resulting from either exposure to formic acid,[3] or exposure to reactive oxygen species during the ionization process.[4-6]

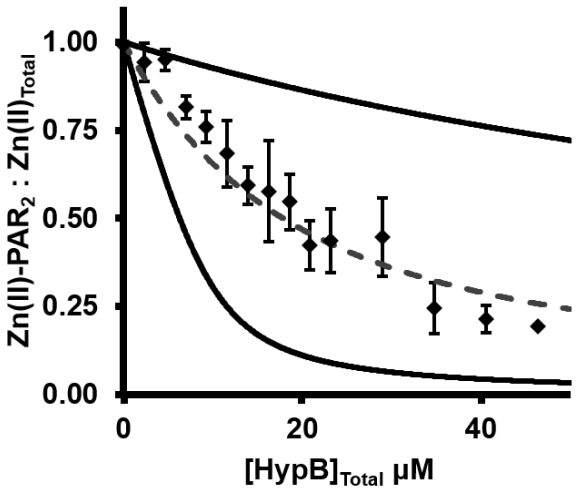

Supplemental Figure 2. Zinc competition experiment between PAR and HypB. Apo-protein was titrated into a solution of 100 μM PAR and 10 μM $ZnSO_4$. The absorbance at 412 nm and 500 nm was monitored and converted to fractional distribution of zinc. Data from three experiments were fit, using a custom DynaFit script, to an average K_d of $(2.2 \pm 0.6)\times10^{-11}$ M. The fractional saturation of the average dissociation constants from three independent experiments (dashed) and fractional saturation from tenfold weaker and tenfold tighter dissociation constants (black) are shown.

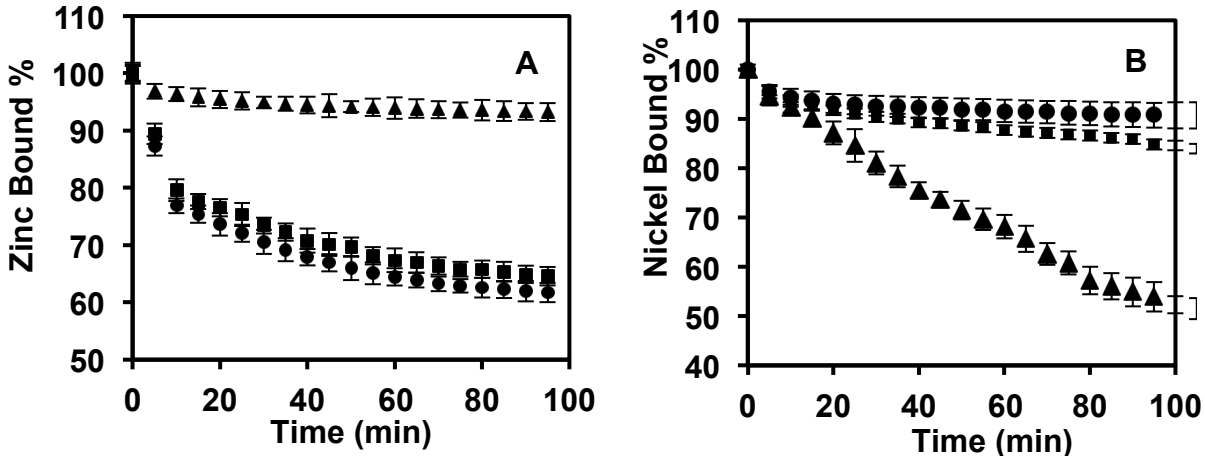

Supplemental Figure 3. SlyD prevents zinc release and accelerates nickel release from HypB. (A) Zn(II)-HypB and (B) Ni(II)-HypB (5 μM) were incubated with 100 μM PAR in the absence (circles) and presence of 50 μM SlyD (triangles) or SlyD146 (squares). Metal release was monitored every 5 min by measuring the absorbance at 495 nm of the metal-PAR_2 complex. The data were converted to percent metal bound.

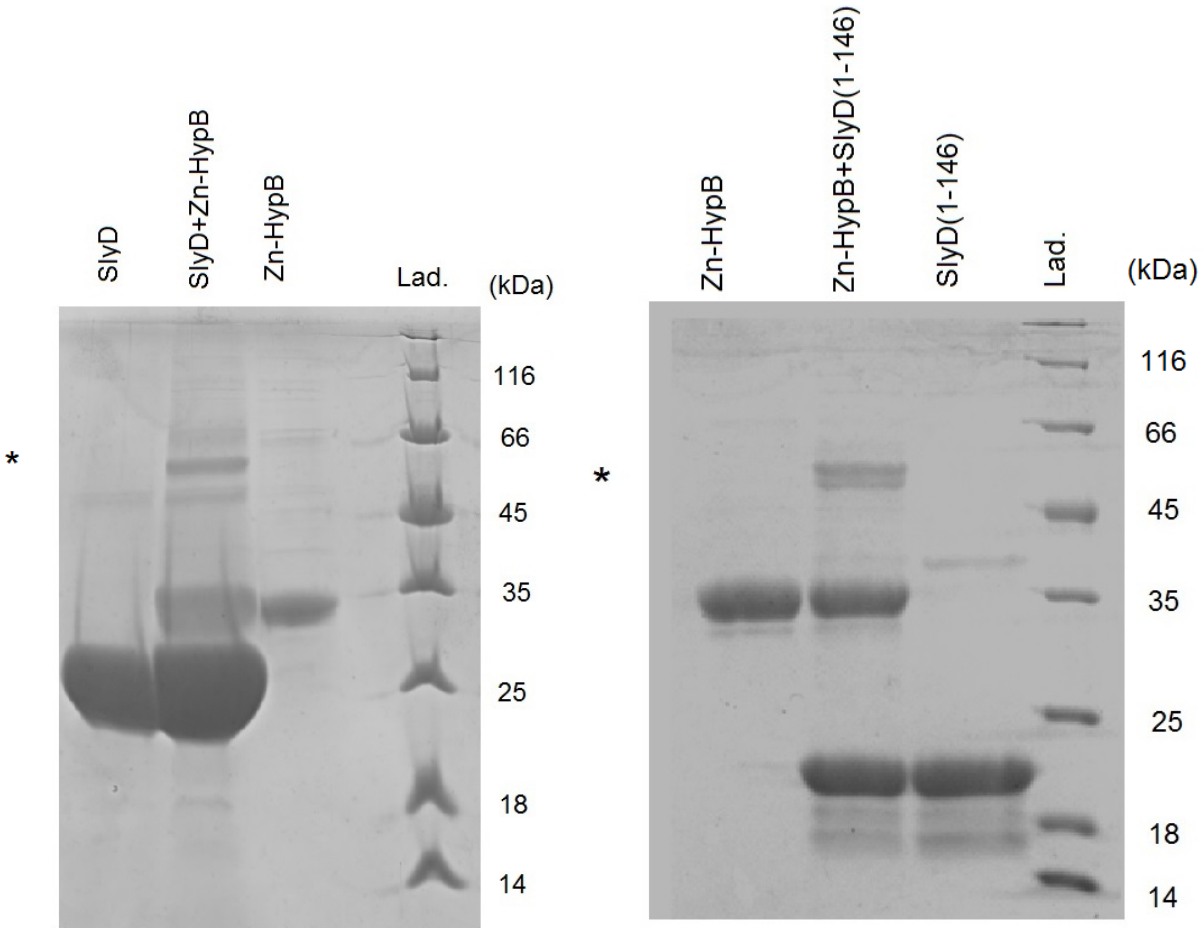

Supplemental Figure 4. Chemical cross-linking of Zn(II)-HypB and SlyD. Zn(II)-HypB (20 μM) was incubated with 80 μM SlyD or SlyD146 at room temperature for 3 h. EDC (5 mM) was added and allowed to react at room temperature for 1 h. The reactions were resolved on 12.5% SDS-polyacrylamide gel and visualized using a coomassie blue stain. Controls with isolated proteins are included. The asterisks indicate the heterodimeric Zn(II)-HypB-SlyD products.

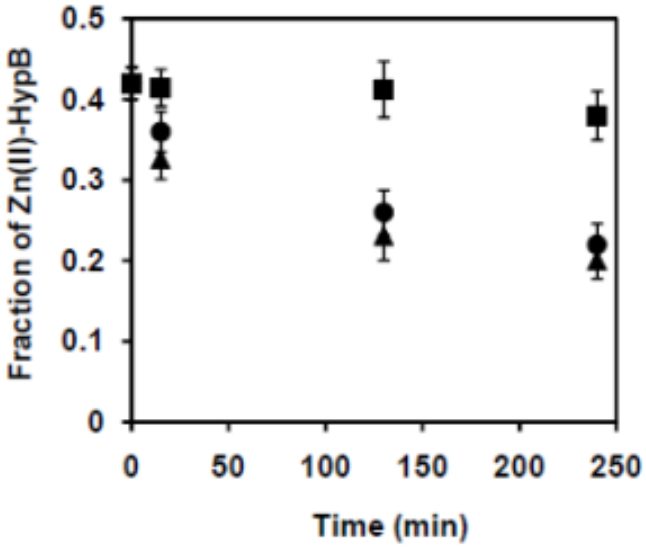

Supplemental Figure 5. Zinc release from HypB HAS monitored by ESI-MS. Zn(II)-HypB (30 μM) was incubated with 1 mM EGTA and analyzed by ESI-MS. Zinc release to EGTA was monitored by determining the fraction of zinc loaded HypB in the absence of SlyD (triangles), or in the presence of 90 μM WT-SlyD (squares), or 90 μM SlyD146 (circles). WT-SlyD was found to block the release of zinc from the HAS of HypB to EGTA. Each data point is an average from at least three independent experiments and the error bars represent one standard deviation.

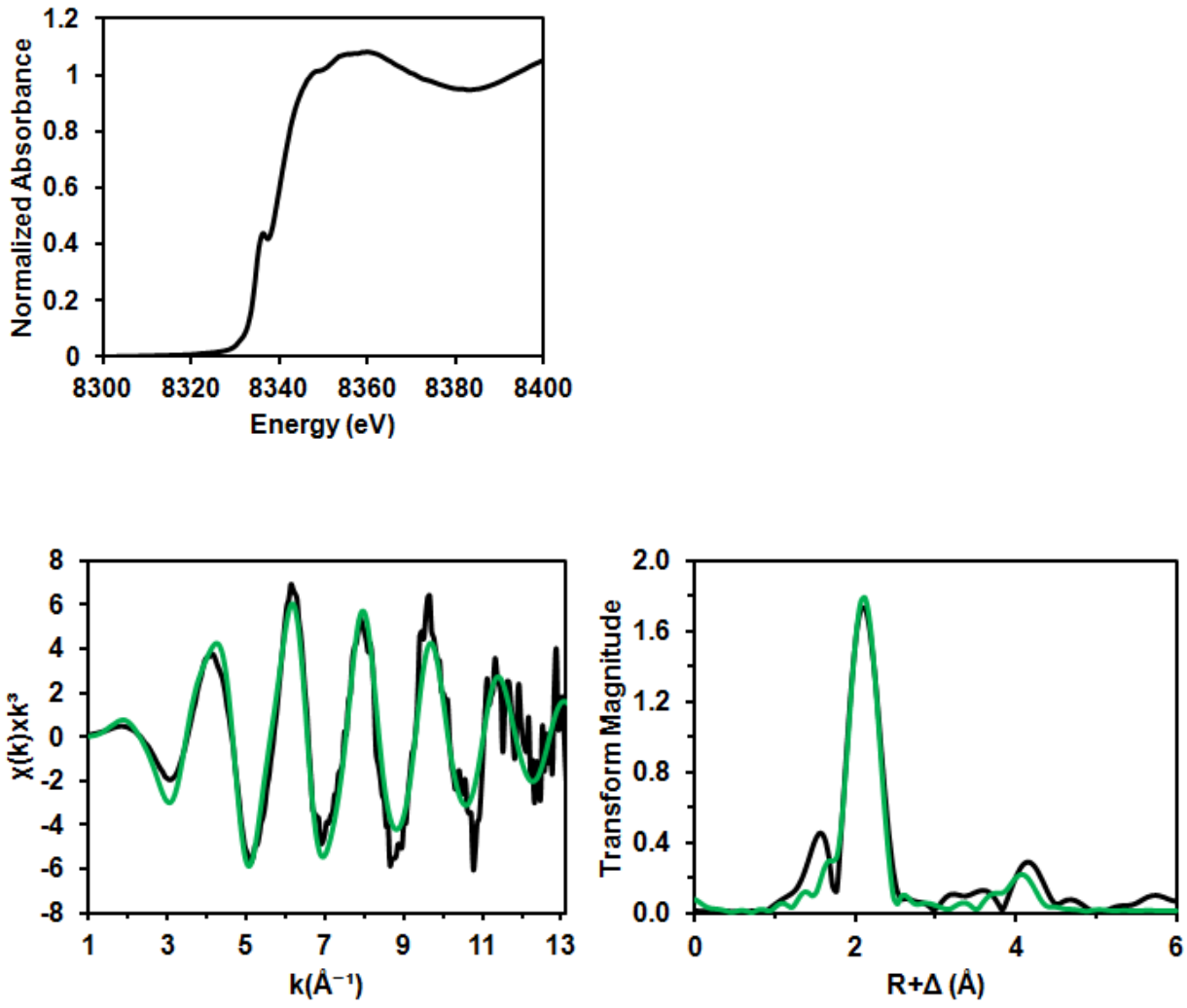

Supplemental Figure 6. XAS of Ni(II)-HypB. (Top) Ni(II) near-edge spectrum of Ni(II)-HypB. HypB loaded with 0.7 equivalents of nickel in the high-affinity site exhibits a 1s-4p_z pre-edge peak at 8336 eV, similar to a previously published spectrum.[7] (Bottom) k^3 weighted Ni(II) EXAFS data (left) and Fourier transform data (right) of HypB (black) loaded with 0.7 equivalents of nickel in the high-affinity site. The best fit model (green) corresponds to a S_3/N coordination environment, similar to previously published data.[7].

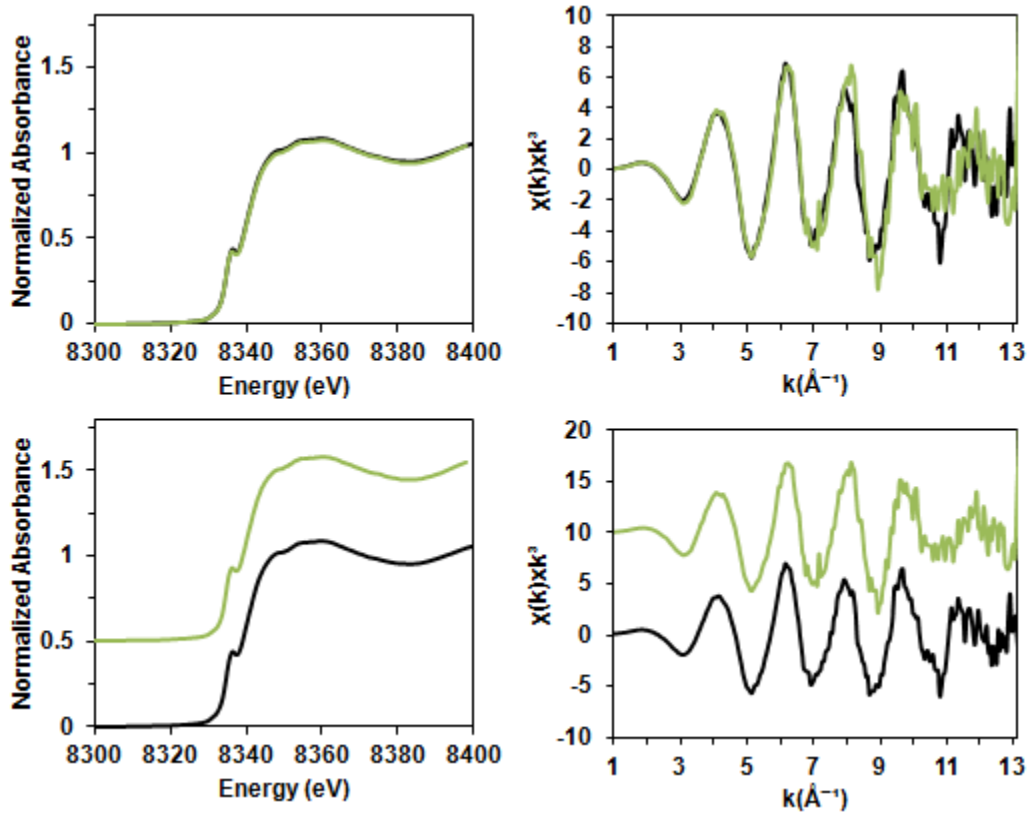

Supplemental Figure 7. XAS of Ni(II)-HypB and Ni(II)-(HypB+SlyD146). The overlays (top) and offset (bottom) of Ni(II) near-edge spectra (left) and k^3 weighted Ni(II) EXAFS (right) of Ni(II)-HypB (black) and Ni(II)-(HypB+SlyD146) (green) are shown. The two sets of spectra are similar, indicating that SlyD146 does not perturb the HypB-Ni(II) site.

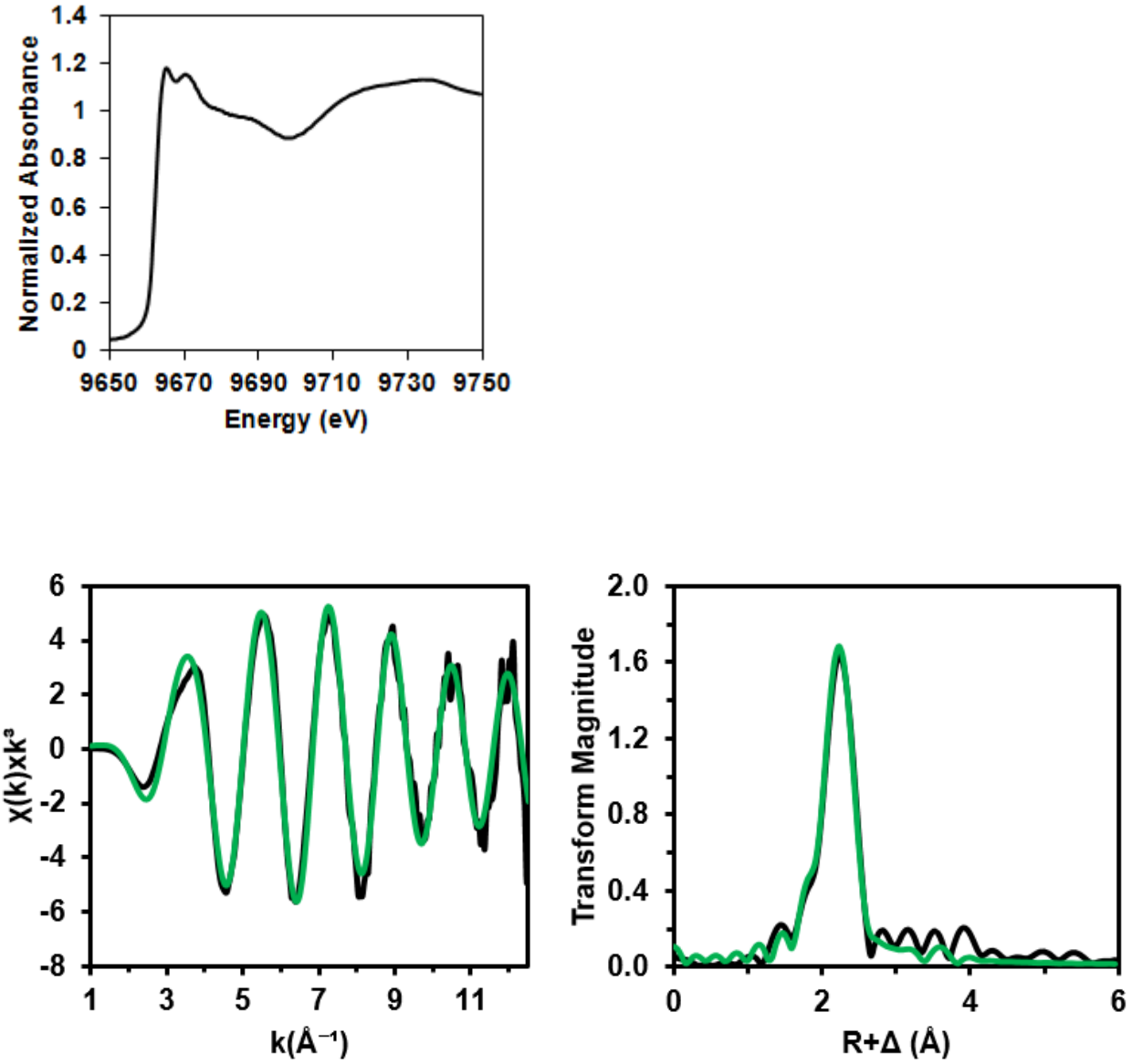

Supplemental Figure 8. XAS of Zn(II)-HypB. (Top) Zn(II) near-edge spectrum of HypB loaded with 0.7 equivalents of zinc. (Bottom) k^3 weighted Zn(II) EXAFS data (left) and Fourier transform data (right) of Zn(II)-HypB (black). The best fit model (green) corresponds to a S_3/N coordination environment.

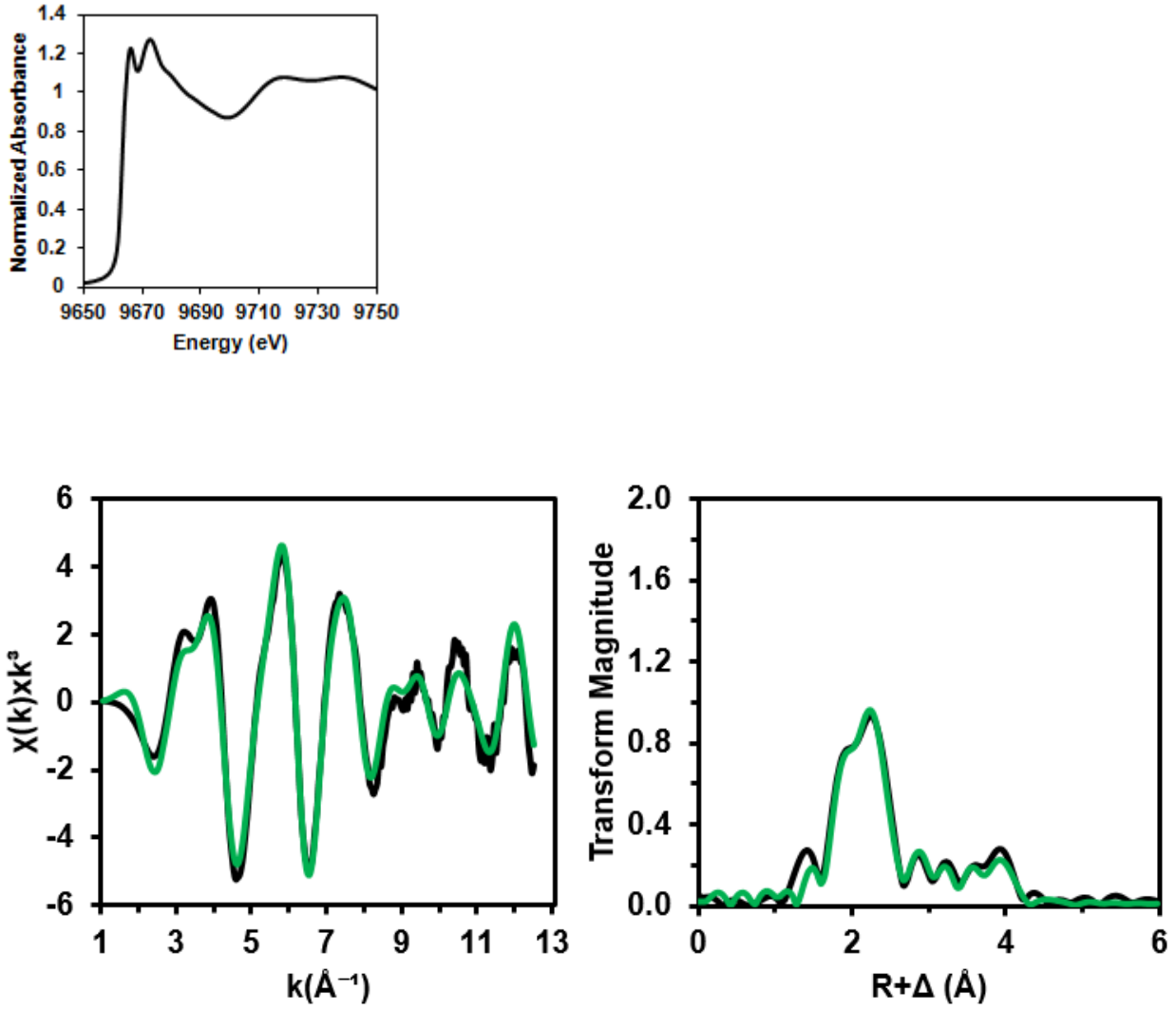

Supplemental Figure 9. XAS of Zn(II)-SlyD. (Top) Zn(II) near-edge spectrum of Zn(II)-SlyD. SlyD was loaded with 0.7 equivalents of zinc. (Bottom) k^3 weighted Zn(II) EXAFS data (left) and Fourier transform data (right) of Zn(II)-SlyD (black). The best fit model (green) corresponds to a S_2/His_2 coordination environment.

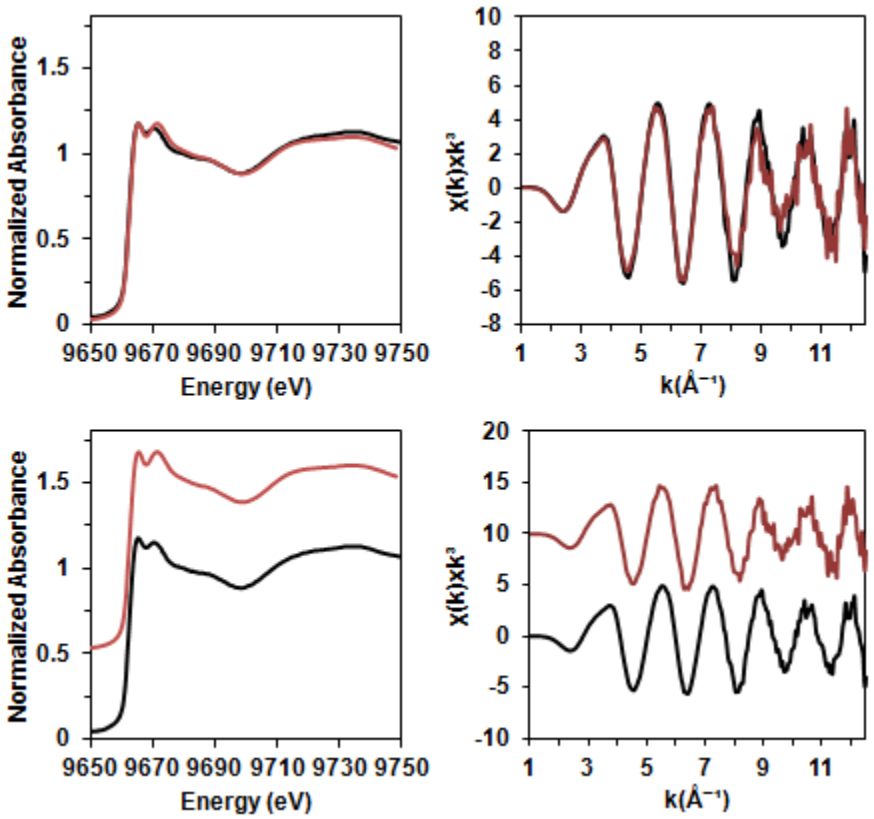

Supplemental Figure 10. XAS of Zn(II)-HypB and Zn(II)-(HypB+SlyD146). The overlays (top) and offset (bottom) of Zn(II) near-edge spectra (left) and k^3 weighted Zn(II) EXAFS (right) of Zn(II)-HypB (black) and Zn(II)-(HypB+SlyD146) (red). The two sets of spectra are similar, indicating that Zn(II)-HypB and Zn(II)-(HypB+SlyD146) have similar coordination environments.

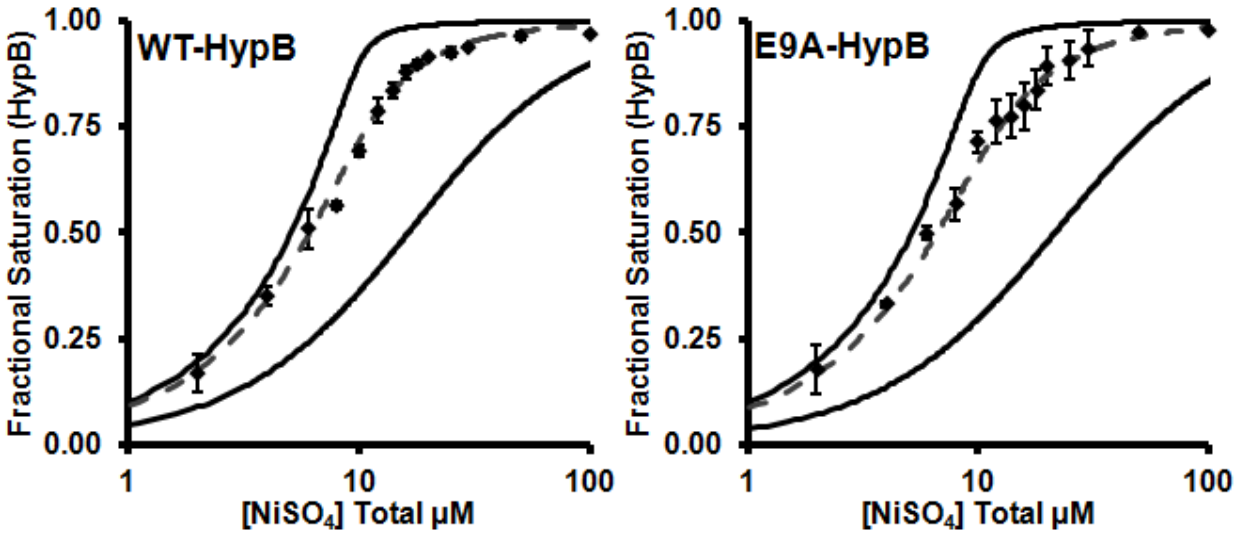

Supplemental Figure 11. Nickel competition experiment between EGTA and WT-HypB or E9A-HypB. Nickel was titrated into a solution of 10 µM apo-protein and 1 mM EGTA. The absorbance at 320 nm was monitored and converted to fractional saturation. Data from three experiments were fit, using a custom DynaFit script, to an average K_d of $(6.0 \pm 0.6)\times10^{-14}$ M and $(9 \pm 4)\times10^{-14}$ M for WT-HypB and E9A-HypB, respectively. The fractional saturation of the average dissociation constants from three independent experiments (dashed) and fractional saturation calculated from tenfold weaker and tenfold tighter dissociation constants (black) are shown.

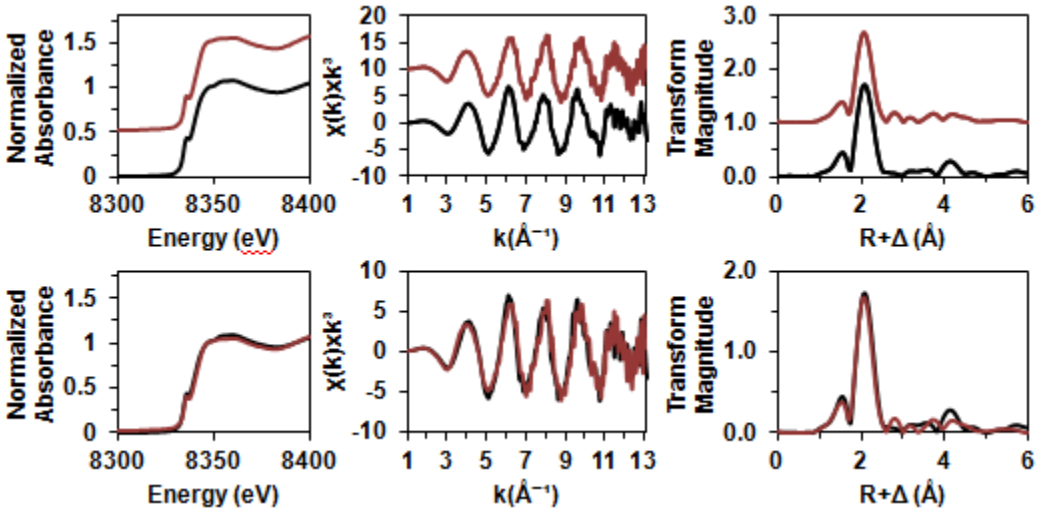

Supplemental Figure 12. Overlay (top) and offset (bottom) of Ni(II) near-edge spectra (left), k^3 weighted Ni(II) EXAFS (middle), and Fourier transform data (right) of Ni(II)-HypB (black) and Ni(II)-E9A-HypB (red). The two sets of spectra are similar, indicating that the E9A mutation does not disrupt the nickel coordination of the HAS.

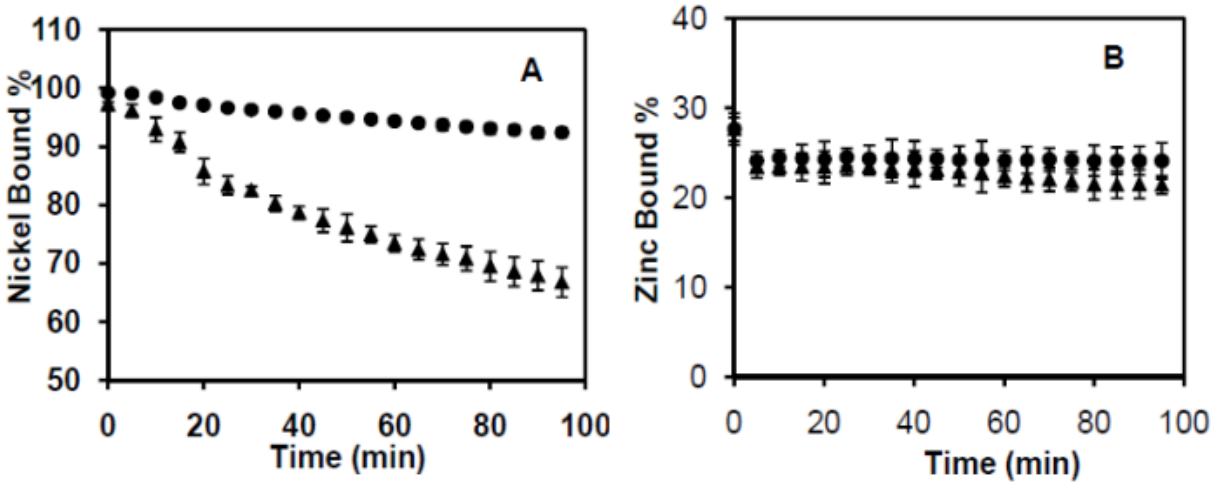

Supplemental Figure 13. E9A-HypB HAS metal release experiments. Ni(II)-E9A-HypB (left) and Zn(II)-E9A-HypB (right) (5 μM) were incubated with 100 μM PAR) in the absence (circle) or presence of 50 μM SlyD (triangle). Metal release was monitored every 5 minutes by measuring the absorbance at 495 nm from the metal-PAR_2 complex. The data were converted to percent metal bound by determining total metal content following treatment of a separate metal loaded protein sample with 100 μM PMB. Each data point is an average from at least three independent experiments and the error bars represent one standard deviation.

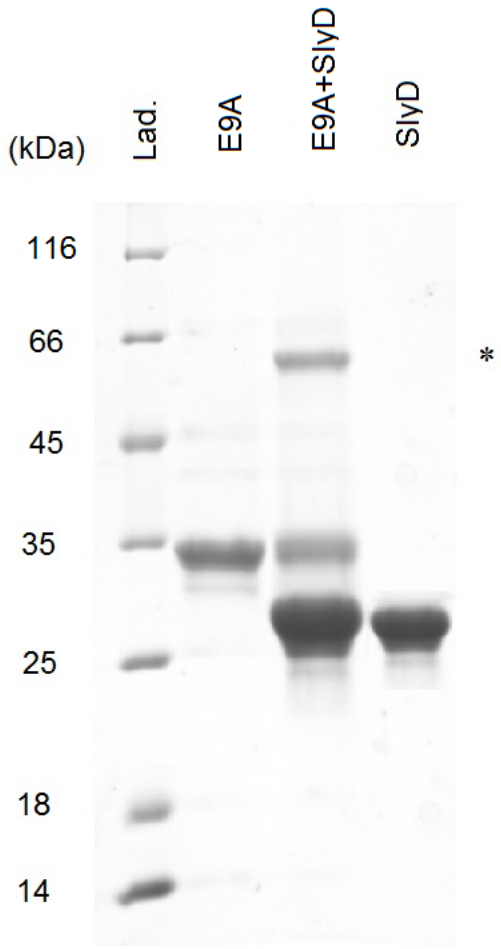

Supplemental Figure. 14. Chemical cross-linking of Ni(II)-E9A-HypB and SlyD. Ni(II)-E9A-HypB (10 μM) was incubated with 50 μM SlyD in an anaerobic glovebox at 4 °C for 2 h. EDC (5 mM) was added to the mixture or to samples containing individual proteins, and the samples were further incubated at room temperature for 1 h. The reactions were resolved on 12.5% SDS-polyacrylamide gel and visualized with a coomassie blue stain. The heterodimeric Ni(II)-E9A-HypB + SlyD cross-linked product is indicated with an *asterisk.*

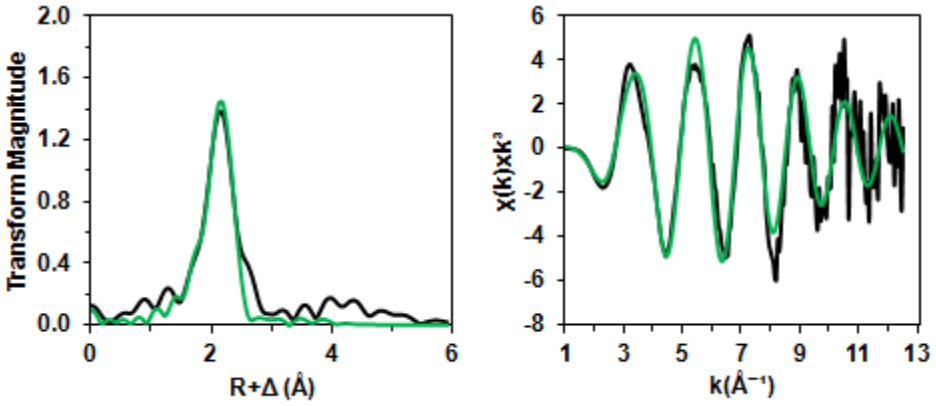

Supplemental Figure 15. Fourier transform data (left) and k^3 weighted Zn(II) EXAFS data (right) of Zn(II)-E9A-HypB (black) loaded with 0.7 equivalents of zinc in the high-affinity site. The best fit model (green) corresponding to a S_3/N_2 coordination environment.

Supplemental Tables

Supplemental Table 1. Ni(II) and Zn(II) EXAFS Curve-fitting results.

Sample Description	A-Bs	N	R (Å)	σ^2 (Å^2)	ΔE_0 (eV)	F-factor
Ni(II)-HypB	Ni-S	4	2.189(4)	0.0052(2)	-7.4(7)	0.378
	Ni-S	**3**	**2.186(5)**	**0.0054(2)**	**-7.0(7)**	**0.349**
	Ni-N	**1**	**2.035(5)**	**0.0029(2)**		
	Ni-S	2	2.214(4)	0.0041(4)	-3.8(6)	0.354
	Ni-N	2	2.025(6)	0.002(3)		
	Ni-S	1	2.243(6)	0.0011(5)	0.0(7)	0.372
	Ni-N	3	2.036(5)	0.0011(4)		

Sample Description	A-Bs	N	R (Å)	σ^2 (Å^2)	ΔE_0 (eV)	F-factor
Ni(II)-E9A-HypB	Ni-S	4	2.165(4)	0.0069(3)	-13.1(8)	0.477
	Ni-S	**3**	**2.162(6)**	**0.0051(5)**	**-11(1)**	**0.403**
	Ni-N	**1**	**2.078(4)**	**0.0027(4)**		
	Ni-S	2	2.184(5)	0.0041(6)	-6(9)	0.401
	Ni-N	2	2.047(1)	0.0041(7)		
	Ni-S	1	2.211(6)	0.0015(5)	0.0(9)	0.406
	Ni-N	3	2.034(8)	0.003(6)		

Sample Description	A-Bs	N	R (Å)	σ^2 (Å^2)	ΔE_0 (eV)	F-factor
Zn(II)-HypB	Zn-S	4	2.318(2)	0.0058(1)	-10.1(0)	0.274
	Zn-S	**3**	**2.324(3)**	**0.0039(1)**	**-7.0(1)**	**0.2377**
	Zn-N	**1**	**2.066(2)**	**0.0073(1)**		
	Zn-S	2	2.338(2)	0.0011(1)	-8.4(5)	0.209
	Zn-N	2	2.087(5)	0.0023(4)		
	Zn-S	2	2.339(4)	0.001(2)	-7.7(7)	0.317
	Zn-His	3	2.067(4)	0.0012(2)		
	Zn-N	2	2.103(7)	0.002(2)		
	Zn-S	1	2.359(2)	-0.0019(1)	0.0(5)	0.218902
	Zn-N	3	2.128(4)	0.002(3)		

Sample Description	A-Bs	N	R (Å)	σ² (Å²)	ΔE_0 (eV)	F-factor
Zn(II)-E9A-HypB	**Zn-S**	**3**	**2.306(6)**	**0.0053(3)**	**-15(2)**	**0.403**
	Zn-N	**2**	**2.063(2)**	**0.0072(6)**		
	Zn-S	2	2.306(3)	0.0029(5)	-14.7(5)	0.467
	Zn-N	3	2.176(5)	0.0052(5)		
	Zn-S	3	2.308(6)	0.0055(4)	-15(2)	0.422
	Zn-N	2	2.072(9)	0.007(7)		
	Zn-S	3	2.302(6)	0.0058(4)	-14(6)	0.407
	Zn-N	3	2.109(2)	0.0145(8)		
	Zn-S	3	2.298(5)	0.0052(3)	-16(4)	0.426
	Zn-N	1	2.052(2)	0.0103(3)		

Sample Description	A-Bs	N	R (Å)	σ² (Å²)	ΔE_0 (eV)	F-factor
Zn(II)-SlyD	Zn-S	3	2.279(6)	0.0089(5)	-7.0(3)	0.446
	Zn-N	1	2.007(4)	0.0098(5)		
	Zn-S	3	2.266(9)	0.0055(5)	-11.4(5)	0.453
	Zn-His	1	1.99(8)	0.0034(6)		
	Zn-S	**2**	**2.297(4)**	**0.0042(3)**	**-10.9(7)**	**0.211**
	Zn-His	**2**	**2.007(5)**	**0.0022(4)**		
	Zn-S	2	2.297(4)	0.0042(3)	-10.9(7)	0.351
	Zn-N	2	2.007(5)	0.0022(4)		
	Zn-S	2	2.29(4)	0.0043(3)		
	Zn-His	1	1.97(16)	0.0014(6)	-11.7(8)	0.356
	Zn-N	1	2.02(19)	0.0016(3)		

[a] A-Bs denotes absorber and backscatterer interaction; N denotes coordination number; R is given in Å and represents interatomic distances; σ^2 given in $Å^2$, are the Debeye-Waller factors (mean-square deviations in interatomic distance); the threshold energy shifts, ΔE_0 are given in eV. The values in parentheses are the estimated standard deviations obtained from the diagonal elements of the covariance matrix. The F-factor or fit-error function is defined as $(\Sigma k^6(\chi(k)_{calcd} - \chi(k)exptl)^2 / \Sigma k^6 \chi(k)_{exptl}^2)^{1/2}$. The summation is over all data points included in the refinement. [b] The best fit models are bolded.

References

1. S. M. Kelly, T. J. Jess and N. C. Price, How to study proteins by circular dichroism, *Biochim. Biophys. Acta*, 2005, **1751**, 119-139.
2. M. R. Leach, J. W. Zhang and D. B. Zamble, The Role of Complex Formation between the *Escherichia coli* Hydrogenase Accessory Factors HypB and SlyD, *J. Biol. Chem.*, 2007, **282**, 16177-16186.
3. J. P. Whitelegge, in *HPLC of Peptides and Proteins: Methods and Protocols*, ed. M.-I. Aguilar, Springer New York, Totowa, NJ, 2004, pp. 323-339.
4. B. L. Boys, M. C. Kuprowski, J. J. Noël and L. Konermann, Protein Oxidative Modifications During Electrospray Ionization: Solution Phase Electrochemistry or Corona Discharge-Induced Radical Attack?, *Anal. Chem.*, 2009, **81**, 4027-4034.
5. L. Wang and M. R. Chance, Structural Mass Spectrometry of Proteins Using Hydroxyl Radical Based Protein Footprinting, *Anal. Chem.*, 2011, **83**, 7234-7241.
6. H. Kaluarachchi, J. F. Siebel, S. Kaluarachchi-Duffy, S. Krecisz, D. E. K. Sutherland, M. J. Stillman and D. B. Zamble, Metal selectivity of the *Escherichia coli* nickel metallochaperone, SlyD, *Biochemistry*, 2011, **50**, 10666-10677.
7. A. V. Dias, C. M. Mulvihill, M. R. Leach, I. J. Pickering, G. N. George and D. B. Zamble, Structural and biological analysis of the metal sites of *Escherichia coli* hydrogenase accessory protein HypB, *Biochemistry*, 2008, **47**, 11981-11991.